Monte Carlo simulation of the property of a scintillation bar in the multi-neutron correlation spectrometer*

SONG Yu-Shou(宋玉收)[1)] YE Yan-Lin(叶沿林)[2)] GE Yu-Cheng(葛愉成) LÜ Lin-Hui(吕林辉)
Faisal Q.(曲乐实) JIANG Dong-Xing(江栋兴) HUA Hui(华辉) ZHENG Tao(郑涛)
LI Zhi-Huan(李智焕) LI Xiang-Qing(李湘庆) LOU Jian-Ling(楼建玲) LU Fei(卢飞)
FAN Feng-Ying(范凤英) CAO Zhong-Xin(曹中鑫) LI Qi-Te(李奇特) XIAO Jun(肖军)

(School of Physics and State Key Laboratory of Nuclear Physics and Technology, Peking University, Beijing 100871, China)

Abstract To perform a kinematically complete measurement of the dissociation reaction for neutron-rich nuclei, a multi-neutron correlation spectrometer is proposed at Peking University. A Monte Carlo simulation code based on GEANT4 is developed for a single scintillation bar which processes not only the energy deposition but also the light propagation in the scintillator and the light collection and conversion to signal at the end of the bar in a realistic way. The simulating method is described in detail in this paper, and the timing and position resolutions and detector efficiency are studied based on the simulation and compared with the experimental results. A new method of crosstalk rejection has been demonstrated to be important for the design of the whole spectrometer.

Key words neutron wall, Monte Carlo simulation, neutron halo

PACS 29.30.Aj

1 Introduction

In many cases a neutron rich unstable nucleus can be described as a charged core plus a number of valence neutrons[1]. In breakup or knockout experiments which are often performed to study the weakly binding unstable nuclei, a core fragment and several neutrons fly out at forward angles in the final state. To make an inclusive measurement, a highly efficient, position-sensitive neutron detector system is needed, together with the telescopes used to detect the charged fragments . If the produced neutrons are more than one, e.g. two, the system is required to have the ability to distinguish the real coincidence of the multi-neutrons from the crosstalk which occurs when a neutron gives several signals in the detection system[2, 3]. Existing neutron detector systems of this type are mostly composed of several scintillator walls[4—6]. The crosstalk from the detector modules in different walls (different-wall crosstalk) can partially be eliminated by the kinetic energy filter, the time of flight (TOF) filter, etc[3, 4]. However, these methods also cause a loss of 50% real two-neutron coincidence events while rejecting the crosstalk[7].

Based on the principle described in Refs. [2, 3], a Multi-Neutron Correlation Spectrometer (MNCS) at Peking University is proposed for detection of neutrons at a few MeV to ∼100 MeV. MNCS is aimed at tracking the neutron scattering history in the detector system to provide more efficient crosstalk identification filters. The criterion is to eliminate the crosstalk as much as possible and in the meantime to keep the coincidence detection efficiency as high as possible. For this purpose a detailed simulation is important in order to optimize the detection system design. This article will focus on the study of the performance of

Received 15 December 2008

* Supported by National Basic Research Program (973 Program) of China (2007CB815002), National Natural Science Foundation of China (10827505, 10775003, 10475004, 10405001, J0730316)

1) E-mail: songyushou_cn@yahoo.com.cn

2) E-mail: yeyl@pku.edu.cn (corresponding author)

one module which is the base for the whole system design.

A module of MNCS is firstly designed to consist of two closed packed plastic scintillation (BC408) bars, each with dimensions of 200 cm × 6 cm × 3 cm (length×height×thickness). The two ends of the bar are coupled to XP2020 photo-multiplier tubes (PMT), namely PMT_L and PMT_R. The signal from a PMT is sent to TDC and QDC. According to the difference between the tdc_L (TDC value from PMT_L) and tdc_R (TDC value from PMT_R), the hitting position is obtained. The difference between the average of two TDCs of a bar and the starting timing signal taken from detectors around the target gives the neutron TOF. The energies deposited by ions generated in the reaction induced by the incident neutrons are recorded by QDC (qdc_L and qdc_R, respectively), which are used to track the scattered neutrons. A Monte Carlo simulation based on GEANT4 is developed in this work to follow processes such as neutron-nucleus reaction, energy deposition, light generation and propagation, light collection by PMT and signal conversion.

In this article the simulation method is described in Section 2. The results and discussion are presented in Section 3, including the detection efficiency, time and position resolution of a single scintillator bar, and the possible performance of neutron tacking and crosstalk rejection. A summary is given in Section 4.

2 Simulation method

2.1 Detector Definition

In this simulation, the coordinate is set up as follows: The origin point is at the geometrical center of the scintillator bar; the x axis is along the bar from right to left, the y axis points upwards and the z axis is along the beam direction. In the concrete class of G4VUserDetectorConstruction[8, 9], the geometry of the scintillator bar is constructed as a box with dimensions of 200 cm × 6 cm × 3 cm. The bulk properties of BC408 are defined according to Table 1[10]. The bar is configured as a sensitive detector to watch physical reactions, providing information such as energy deposition, particle production and light generation. In practice the surface of the scintillator bar is well polished and wrapped with Tyvek paper[11]. Therefore, in the simulation code the surface (optical) of the bar is set 'polishedbackpainted'[12]. Because GEANT4 does not implement the PMT device, two glass cylinders with the same dimensions as XP2020 PMT are placed at both ends of the bar. The two cylinders are set as sensitive detectors to record the arrival time of the scintillation light (described in detail in the following sections). The bar and the photon collectors (glass cylinders) are usually coupled by silicon grease with a similar refraction index (1.5) to glass. Hence, in the code the optical surface between the bar and the photon collector is set as the type 'polished'.

Table 1. Property parameters for the plastic scintillator BC408.

density/(g/cm^3)	1.032
ratio H:C atoms	1.104
refraction index	1.58
light output % anthracene	64
ratio slow component/fast component	0.27
decay time of slow component/ns	14.2
rise time of fast component/ns	0.9
decay time of fast component/ns	2.1
light attenuation length/cm	∼380
wavelength of maximum emission/nm	425

2.2 Physics and optical processes

The basic reaction processes involved in the detector happen between the incident neutrons and the C and H atoms compounding the scintillator material. The neutrons are detected with the scintillation light caused by the energy loss of produced charged particles. This simulation utilizes the built-in GEANT4 physics list QGSP_BERT_HP[9], which uses the Bertini intranuclear cascade model[13] for particles below 10 GeV and a data-driven high precision neutron package for neutrons below 20 MeV down to thermal energies. QGSP_BERT_HP is the recommended physics list for our energy range and has better agreement with the experimental data in comparison with other physics lists, such as LHEP (low and high energy physics)[9, 13], for low and medium energy particles.

Light transmission in the scintillator is implemented by creating an instance of the pure virtual class G4VPhysicsConstructor, where all the relevant processes are assigned to the predefined particle G4OpticalPhoton in GEANT4. Then the G4VPhysicsConstructor module is registered to QGSP_BERT_HP. Thus, we include all the necessary physical and optical processes in the simulation. The relevant optical processes in the simulation are: scintillation light generation, Cerenkov process, optical absorption, optical Rayleigh and optical boundary processes. The dominant photon-generating process is the scintillation according to the BC408 specifica-

tion. The absolute light output for electrons in BC408 is given in Table 1. According to the relative light response curves[10] (Fig. 1) and the absolute light output of electrons, the light output for other charged particles (protons, deuterons, tritons, alphas and so on) can be fitted by a polynomial function $f_{\rm L}(E_{\rm k})$, where $E_{\rm k}$ is the kinetic energy of the charged particle. Within each G4Step, assuming the kinetic energy at the previous point is $E_{\rm pre}$ and the total energy deposit $E_{\rm dep}$, the light output in the present step is:

$$N_{\rm step} = f_{\rm L}(E_{\rm pre}) - f_{\rm L}(E_{\rm pre} - E_{\rm dep}) . \quad (1)$$

For other heavy charged particles other than those mentioned above (^{12}C for instance), the light response is very weak and its contribution is ignored. In the scintillation class, both the fast and slow light components could be generated according to the ratio provided by the user. The photons are generated according to an exponential timing distribution with the given decay constant. The direction of the photons is created isotropically. The attenuation length is used to randomly absorb the light. The reflection and refraction at the boundary are treated according to the surface definition.

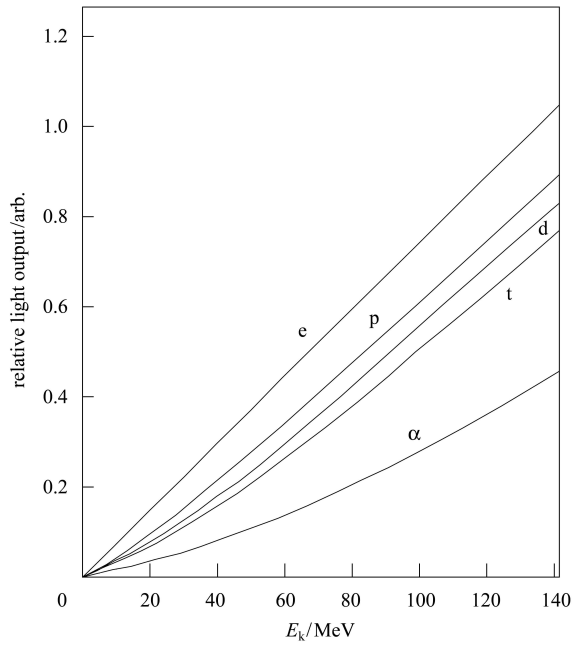

Fig. 1. The relative light response for electrons, protons, deuterons, tritons and alpha particles with different kinetic energy ($E_{\rm k}$) in BC408 scintillator.

2.3 Signal digitization

At the PMT photocathode, photoelectrons (PE) are produced based on the quantum efficiency. To save the computer CPU time, photon tracks are killed in G4StackingAction class with a survival probability of the quantum efficiency (20%). For each primary photoelectron, the multiplicity effect happens in a period of the PMT transit time $t_{\rm trans}$ before being collected by the PMT anode. The average signal arrival time at the anode is

$$t_{\rm anode} = t_{\rm cathode} + t_{\rm trans} . \quad (2)$$

The signal at the PMT anode corresponding to a single photoelectron is simulated by a time response function[14]

$$V_i(t) = \frac{GC_{\rm e}}{C_{\rm c}} \frac{t^2 {\rm e}^{-t^2}/\tau^2}{\int t^2 {\rm e}^{-t^2}/\tau^2 {\rm d}t} . \quad (3)$$

where G is the gain factor of the PMT, $C_{\rm e}$ the conversion factor for charge to voltage, $C_{\rm c}$ the coupling capacity, and τ the rise time of the PMT. The final output of a PMT is then the convolution of all the photoelectron signals

$$V_{\rm PMT}(t) = \sum_i V_i(t) . \quad (4)$$

The time bin size of the signal is set to be 20 ps, which is actually the timing resolution of the TDC. With the PMT signal, we extract the timing (TDC) value by the constant-fraction discrimination method, whereas the charge output (QDC) is obtained by the time integral of the signal. The parameters for PMT used in the present simulation are listed in Table 2.

Table 2. Parameters of PMT used in the simulation.

quantum efficiency	20%
rise time/ns	1.6
gain	3.7×10^7
transit time/ns	28.0
TDC time resolution/ps	20
coupling capacitor/pC	200
conversion factor of charge to voltage	1

3 Results and discussion

3.1 The performance of a single scintillation bar

Firstly, we study how the hit position affects the time resolution. As indicated above, the dimensions of the scintillator are 200 cm × 6 cm × 3 cm which is exposed to the incident neutron at 80 MeV. When neutrons hit the center point of the scintillator, the distribution of $t_{\rm L}$ versus $q_{\rm L}$ is shown in Fig. 2(a), where $t_{\rm L}$ and $q_{\rm L}$ are the TDC and QDC values respectively, for a left PMT$_{\rm L}$. Even though the constant fraction discrimination method is used, the time resolution still varies with the light output amplitude

(QDC), which reflects the statistical property of the scintillation photons. The time resolution for signals above 1 MeV electron equivalent (1 MeVee) threshold is $\sigma_{\rm L}=(86\pm2)$ ps as shown in Fig. 2(b). Similarly we get the time resolution of $\rm PMT_R$ $\sigma_{\rm R}=(84\pm2)$ ps. In order to compare with the experimental results, the weighted average time $t_{\rm av}$ is expressed as

$$t_{\rm av}=\frac{t_{\rm L}\sigma_{\rm R}^2+t_{\rm R}\sigma_{\rm L}^2}{\sigma_{\rm R}^2+\sigma_{\rm L}^2} \quad (5)$$

and the corresponding time resolution is $\sigma_{\rm av}=(80\pm2)$ ps. When taking an average propagation velocity v of about 17.0 cm/ns[11] this timing resolution corresponds to a position ($x=v(t_{\rm L}-t_{\rm R})/2$) resolution of about 1 cm. Of course the simulation just gives the lower limit of the resolution coming purely from the statistical fluctuation. If the radiation background and the electronics noise are taken into account, the timing as well as the position resolution are normally a few times worse than the above lower limit values, depending on the real experimental situation.

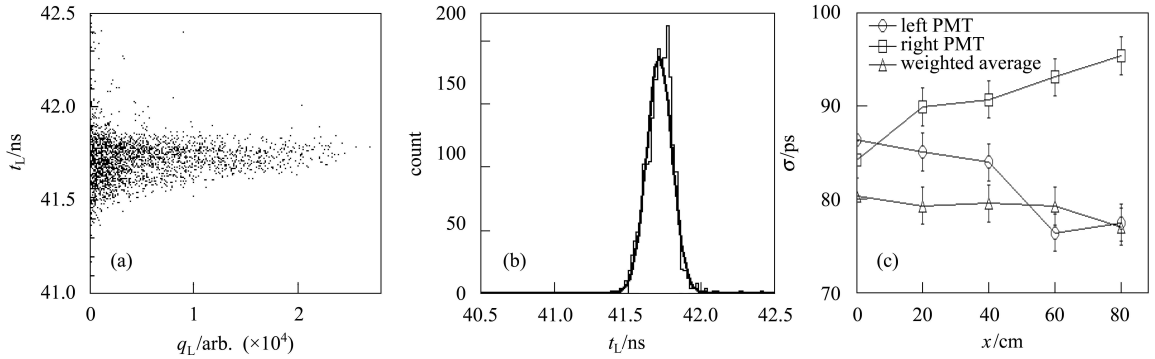

Fig. 2. (a) The correlation between TDC and QDC of a left PMT. (b) The timing spectrum given by a left PMT. (c) The time resolution of a scintillation bar as a function of hit position starting from the center point (x=0) to the left end of the scintillator, where the error bar comes from Gaussian fitting.

When we move the neutron hit position from the center point to the left end of the bar, the time resolution varies as shown in Fig. 2(c). This variation agrees with the experimental data[10, 15] within the error bar.

MNCS is proposed to cover an angle range of $\pm5^\circ$ in the y direction and $\pm10^\circ$ in the x direction at a distance of ~5 m downstream of the target. Scintillation bars with dimensions of 200 cm × 6 cm × 3 cm placed horizontally or with dimensions of 100 cm × 6 cm × 3 cm placed vertically can either form such a detector matrix. According to our simulation, the difference of time resolution and detection efficiency between the two kinds of scintillator bars is very small (below 3%). Therefore the first option with a longer bar and two times fewer PMTs is adopted. In order to increase the detection efficiency we might double the thickness of the scintillator bar. However, the time resolution gets much worse and the precision to determine the flight distance for neutron TOF is doubled too. Therefore a compromise to improve the efficiency while keeping the same resolution performance is to stack two bars of 200 cm × 6 cm × 3 cm together to make one module of 6 cm in thickness.

The detection efficiency and time resolution of a single scintillation bar are investigated against different neutron energies. To test the validation of the simulation relative to the existing experimental results, the incident neutron energies at $E_{\rm n}=7.1$ MeV and $E_{\rm n}=12.7$ MeV are firstly selected. The efficiency values (ε) of a scintillation bar at these neutron energies for a threshold at 0.25 MeVee are 12.5% and 10.5%, respectively. These values for a stacked module of 6 cm in thickness are 19.9% and 23.4%, respectively, which agree with the experimental results of 22.7% and 27.4%[17] within the error bar. The detection efficiency at 3 MeV neutrons (21.6% for a threshold at 0.25 MeVee) also agrees with the experimental result[11]. We can then extend the calculation to higher neutron energies. As shown in Fig. 3, the time resolution improves while the detection efficiency decreases with increasing neutron energies. It is clear that the higher the neutron energy is, the more layers of scintillator are needed to reach the similar detection efficiency. Fig. 3 also shows the influence of the detection threshold. The time resolution is almost independent of the threshold while the detection efficiency decreases greatly on increasing the threshold especially at low neutron energies. For our applica-

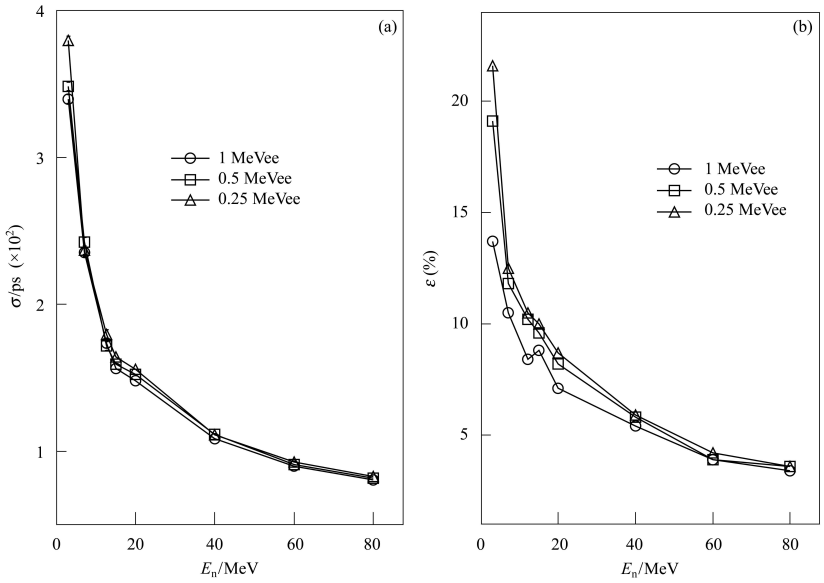

Fig. 3. (a) The average timing resolution and (b) The detection efficiency ε of a single scintillation bar, as a function of incident neutron energy and detection threshold (inner box).

tion at relatively higher energies of 50 — 100 MeV, the threshold could be set at higher values to suppress possible noise without diminishing the detection efficiency.

3.2 The identification of crosstalk neutrons

The neutron signals produced in a plastic scintillator come mostly from (n, p) scattering. The scattered neutrons might cause another signal in different neutron detector modules, which is the so-called crosstalk[2, 3] (CT), and results in a fake signal of another neutron. In order to correctly determine the multi-neutron correlation, rejection of the CT is essential. CT rejection has been performed based on the TOF technique, but it might achieve only about 50% of the rejection rate[7]. Based on the principle proposed in Refs. [2, 3], the precise measurement of the deposited charge of the recoiled protons in addition to the TOF could provide much better criteria for the rejection of CT. It should be kept in mind that the CT rejection is often related to the reduction of the detection efficiency for real neutron coincidence events. Normally some compromise has to be made when setting the criteria and applying the cuts.

In principle the light produced (Y) is proportional to the energy loss $\Delta E_{\rm pe}$ of the recoiled proton:

$$Y = k\Delta E_{\rm pe}\,, \tag{6}$$

where k is a proportional constant. In a long scintillation bar the light attenuation obeys an exponential law. Therefore, values of $\mathrm{QDC_L}$ and $\mathrm{QDC_R}$ can be written as

$$q_{\rm L} = k_{\rm L} Y {\rm e}^{-x/\lambda}, \quad q_{\rm R} = k_{\rm R} Y {\rm e}^{-(l-x)/\lambda}\,, \tag{7}$$

where λ is the effective attenuation length of the scintillator, l the length of the scintillator bar, x the hitting position and $k_{\rm L}$ or $k_{\rm R}$ the factor of light conversion of the readout system at the left or right end of the scintillation bar. Based on Eq. (6) and Eq. (7), $\Delta E_{\rm pe}$ can be deduced as

$$\Delta E_{\rm pe} = K\sqrt{q_{\rm L} q_{\rm R}}\,, \tag{8}$$

where

$$K = \frac{1}{k\sqrt{k_{\rm L} k_{\rm R} {\rm e}^{-l/\lambda}}}\,, \tag{9}$$

which is independent of x. In an experiment K is acquired via calibration measurement for a certain neutron energy. Consequently the energy loss $\Delta E_{\rm pe}$ at other neutron energies can be obtained according to the calibration and the response curve (Fig. 1). If the recoiled proton is absorbed in a scintillator bar, i.e. $\Delta E_{\rm pe} = E_{\rm pe}$, the scattering angle of the primary neutron can then be deduced according to momentum and energy reservation[2, 3]. Fig. 4(a) shows the angular difference ($\Delta\theta$) between the deduced neutron scattering angle ($\theta_{\rm d}$) and the real one ($\theta_{\rm r}$) given by the G4TrackAction class in the simulation. If we put a cut of $(-5^\circ, 5^\circ)$ on $\Delta\theta$, ~50% crosstalk neutrons can be eliminated. Another half of the events have very different deduced angles compared with the real ones, due basically to the incomplete energy absorption for a recoiled proton in a scintillation bar. Assuming that some veto detectors are installed in front of each neutron detector wall, which might provide the energy of the protons escaping from the upstream wall, the incomplete proton energy could be recovered and the

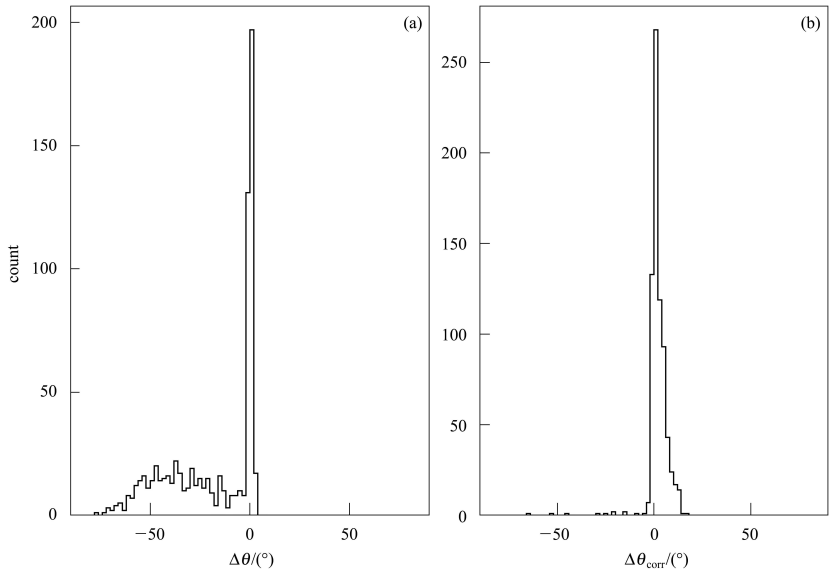

Fig. 4. (a) The difference between the real angle of the scattered neutrons and that calculated according to the light output and n+p scattering kinematics. (b) The angular difference after proton-residual energy correction.

results are shown in Fig. 4(b). In this case a good veto system is also important.

The study of CT rejection here is just preliminary to simply show the working principle. A more realistic simulation should include an analysis of all possible reaction processes in addition to (n, p), treatment of the real time and position resolutions of the scintillation bar, practical configuration of the whole MNCS system, and so on. These studies are underway and will be reported later on.

4 Summary

Using the GEANT4 toolkit, the simulation of neutron detection with a long plastic scintillation bar (BC408) has been performed in detail. With this code, not only the energy deposition but also the light propagation in the scintillator and the light collection and conversion to signal at the end of the bar are processed in a realistic way. One detector module is designed as a close pack of two parallel scintillation bars with dimensions of 200 cm × 6 cm × 3 cm each. The time and position resolutions and detection efficiency of a single scintillation bar for neutron energies below 100 MeV are given. The results are in good agreement with the experimental data. Such results provide a base for optimization of the module design. Furthermore, the principle of a new crosstalk rejection method is demonstrated and the preliminary results show its applicability. Further study of the whole MNCS system design is underway.

References

1 YE Yan-Lin, ZHOU Xiao-Hong, LIU Wei-Ping et al. Chinese Physics C, 2008, **32**: 1
2 Marques F M, Labiche M, Orr N A et al. Nucl. Instrum. Methods A, 2000, **450**: 109
3 WANG J, Galonsky A, Kruse J J et al. Nucl. Instrum. Methods A, 1997, **397**: 380
4 Sakett D, Ieki K, Galonsky A et al. Phys. Rev. C, 1993, **48**: 118
5 Shimoura S, Nakamura T, Ishihara M et al. Phys. Lett. B, 1995, **348**: 29
6 Tilquin I, Masri Y El, Parlog M et al. Nucl. Instrum. Methods A, 1995, **365**: 446
7 Nakamura T, Vinodkumar A M, Sugimoto T et al. Phys. Rev. Lett., 2006, **96**: 252502
8 Allison J, Amako K, Apostolakis J et al. IEEE Trans. Nucl. Sci., 2006, **53**: 270
9 Agostinelliae S, Allisonas J, Amakonucl K et al. Nucl. Instrum. Methods A, 2003, **506**: 250
10 http://www.detectors.saint-gobain.com
11 HU Q Y, YE Y L, LI Z H et al. IEEE Trans. Nucl. Sci., 2005, **52**: 473
12 Knoll G F, Knoll T F, Henderson T U. IEEE Trans. Nucl. Sci., 1988, **35**: 872
13 Titarenko Yu E, Shvedov O V, Batyaev V F et al. 1999, arXiv:nucl-ex/9908012v1
14 Nam J W, Choi Y I, Kim D W et al. Nucl. Instrum. Methods A, 2002, **491**: 54
15 WU Chong, HENG Yue-Kun, ZHAO Yu-Da et al. Nucl. Instrum. Methods A, 2005, **555**: 142
16 Kichimi H, Yoshimura Y, Browder T et al. Nucl. Instrum. Methods A, 2000, **453**: 315
17 Rout P C, Chakrabarty D R, Datar V M et al. Nucl. Instrum. Methods A, 2008, DOI:10.1016/j.nima.2008.09034